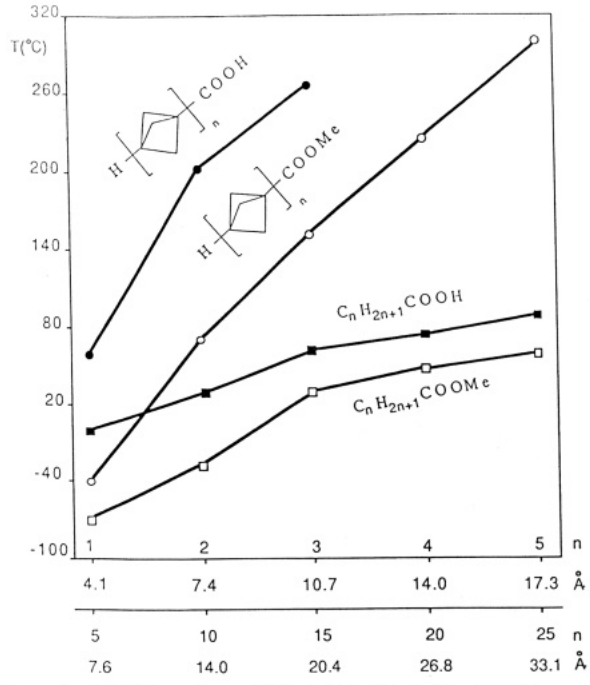

Figure 1. Melting points of (i) **[*n*]2b**, (ii) **[*n*]2a**, (iii) fatty acids $C_nH_{2n+1}COOH$, and (iv) their methyl esters. Horizontal scales give *n* and chain length. The upper one applies to (i) and (ii), the lower one to (iii) and (iv).

monomer ($n = 1$) is formed.[12] At low concentrations of methyl formate and also under anionic polymerization conditions (*n*-butyllithium, 2–25%), practically only **[poly]2** is obtained (unoptimized yield, ~50%).

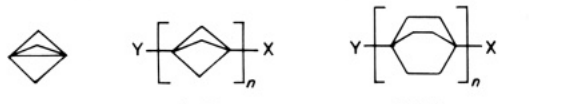

	X	Y		X	Y		X	Y
[*n*]2	**a**, H	COOMe		**f**, H	C(Ph)(COOEt)$_2$		**k**, Br	Br
	b, H	COOH		**g**, H	CH(COMe)COOMe		**l**, PhCH$_2$	Br
	c, H	CH(COOEt)$_2$		**h**, H	CH(CN)COOMe		**m**, SCOMe	SCOMe
	d, H	C(COOEt)$_3$		**i**, H	P(O)(OEt)$_2$			
	e, H	CH(CN)$_2$		**j**, COOH	COOH			

The telomers **[*n*]2** have strikingly high melting points (Figure 1) and remarkable thermal stability up to about 300 °C, considering their high-energy content (the strain energy of bicyclo[1.1.1]pentane is 68 kcal/mol[13]). Differential scanning calorimetry on a sealed sample of **[4]2a** shows a decomposition exotherm at ~320 °C (145.7 kcal/mol). **[poly]2a** decomposes violently at 290 °C with an ~80% weight loss. In keeping with the high melting points, the solubility of the higher telomers is poor, and no solvent for **[poly]2a** was found. Its X-ray diffraction pattern shows a high degree of crystallinity. Its solubility is increased dramatically upon extensive chlorination,[14] and this clearly points the way toward improvements in the solubility of all the telomers.

X-ray structure analysis[15] on **[2]2a** (Figure 2) and **[2]2k** yields an inter-ring C–C bond length of only ~1.48 Å, in keeping with expectations,[16] and a bridgehead–bridgehead separation of ~1.9 Å. In **[3]2m**, obtained[5] by telomerization of **1** with $(CH_3COS)_2$,

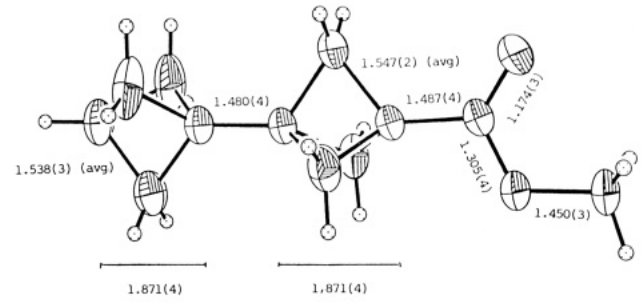

Figure 2. The structure of methyl [2]staffane-3-carboxylate.[14]

the inter-ring distances are even shorter, 1.47 Å.[5] Neighboring staffs are parallel and meshed in the crystal, with axes only 4.6 Å apart. This very efficient packing is undoubtedly responsible for the high melting points.

The salts of the acids **[*n*]2b** are surface active. In the concentration range $c = 1.4 \times 10^{-2}$–3×10^{-4} M, the surface tension[16] of an aqueous solution of the potassium salt of **[3]2b** follows $\gamma = -17.7 \log c - 0.2$ dyn/cm (107 Å^2 of surface area per molecule). Langmuir–Blodgett films have been prepared by using the Cd^{2+} salt of **[4]2b** (45 Å^2/molecule).[18]

The NMR spectra of the "staffs" clearly show each equivalent class of ^1H and ^{13}C nuclei up to $n = 5$. Large bridgehead–bridgehead coupling constants are attributed to transannular orbital interactions,[19] e.g., in **[2]2i**, $^7J[^{31}P^1H] = 1.7$ Hz. The CP-MAS ^{13}C NMR spectrum of **[poly]2a** consists of a peak at δ 50.8 (bridge), a sharp peak at δ 40.3 (bridgehead), and weak end-group signals at δ 169.7 (carbonyl) and δ 27.8 (methine).

Acknowledgment. This work was supported by the National Science Foundation (CHE 8796257) and The Robert A. Welch Foundation (F-1068). We are grateful to Prof. W. H. Wade for permission to use his spinning drop apparatus and to Dr. A. Orendt for a measurement of CP-MAS NMR in the laboratory of Prof. D. M. Grant.

(12) Wiberg, K. B., private communication.
(13) Wiberg, K. B. *Angew. Chem., Int. Ed. Engl.* **1986**, *25*, 312.
(14) Robinson, R. E.; Michl, J., unpublished results.
(15) Obtained by Vincent Lynch. $C_{12}H_{16}O_2$, monoclinic $P2_1/m$ (no. 11) $a = 5.793$ (2) Å, $b = 8.690$ (3) Å, $c = 11.111$ (2) Å, $\beta = 96.13$ (1)°, $V = 556.2$ (3) Å^3, D(calcd) = 1.15 g-cm^{-1} for $Z = 2$, μ(Mo Kα) = 0.7155 cm^{-1}. A total of 2735 reflections (1367 unique reflections, $R_{INT} = 0.0226$) using the ω scan technique with a scan range of 1° in ω from $4 < 2\theta < 50°$. Of these, 971 were considered observed [$F_o \geq 4(\sigma(F_o))$]. The data were corrected for LP, absorption, and decay. The structure was solved by direct methods and refined by full-matrix least-squares procedures to a final $R = 0.0680$ and $R_w = 0.0606$. Collected on a Syntex $P2_1$ diffractometer at 163 K.
(16) Ermer, O.; Lex, J. *Angew. Chem., Int. Ed. Engl.* **1987**, *26*, 447.
(17) Measured by the spinning drop technique.
(18) Yang, H. C.; Bard, A. J.; Michl, J., unpublished results.
(19) Barfield, M.; Della, E. W.; Pigou, P. E. *J. Am. Chem. Soc.* **1984**, *106*, 5051 and references therein.

The Role of Oxygen in the Partial Oxidation of Methane over a Samarium Oxide Catalyst

Alfred Ekstrom* and Jacek A. Lapszewicz

CSIRO Division of Fuel Technology, Lucas Heights Research Laboratory, Private Mail Bag 7 Menai, NSW, 2234, Australia

Received March 17, 1988

The reaction of methane with oxygen at high temperatures to form higher hydrocarbons such as ethane and ethylene was first reported by Ito et al.,[1] who used a lithium-doped magnesium oxide catalyst and suggested that the reaction involved the formation of methyl radicals on Li^+O^- sites and their subsequent gas-phase dimerization. The reaction presents an intriguing mechanistic problem, particularly as it is now known to be catalyzed by a wide range of materials.[2] Samarium oxide appears to be one of the most active catalysts.[3] Details of the reaction mechanism are obscure at present, but it is obvious that the formation of C2 hydrocarbons at these high temperatures in the presence of oxygen

(1) Ito, T.; Wang, J.-X.; Lin, C.-H.; Lunsford, J. H. *J. Am. Chem. Soc.* **1985**, *107*, 5062.
(2) (a) Aika, K.; Moriyama, T.; Takasaki, N.; Iwamatsu, E. *J. Chem. Soc., Chem. Commun.* **1986**, 1210. (b) Bytyn, W.; Baerns, M. *Appl. Catal.* **1986**, *28*, 199. (c) Sofranko, J. A.; Leonard, J. J.; Jones, C. A. *J. Catal.* **1987**, *103*, 302. (d) Otsuka, K.; Jinno, K.; Morikawa, A. *J. Catal.* **1986**, *100*, 353.
(3) Otsuka, K.; Jinno, K.; Morikawa, A. *Chem. Lett.* **1985**, 499.

0002-7863/88/1510-5226$01.50/0

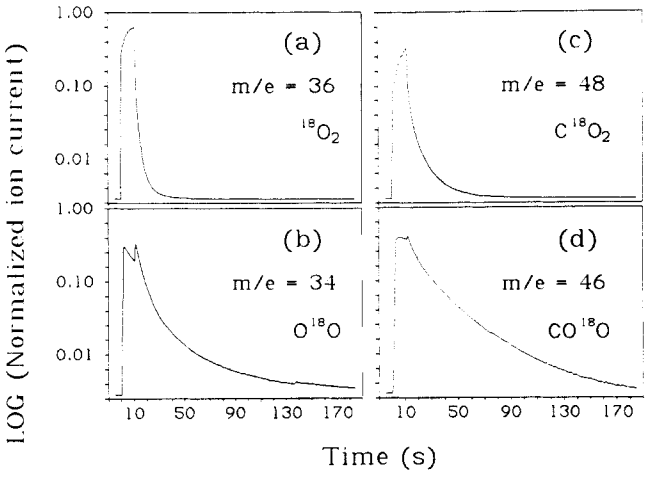

Figure 1. Comparison of the oxygen isotope transients observed when $^{18}O_2$ replaced $^{16}O_2$ in helium (a and b) and the labeled CO_2 transients in methane (c and d). The samarium oxide catalyst was at 700 °C, the oxygen flow was 12.7 cc/min, the helium or methane flow 129 cc/min, giving a total space velocity of 4.7 l/min/g. The switch to $^{18}O_2$ was made at "zero" time, the return to the normal isotope 14 s later.

must be controlled by kinetic rather than equilibrium considerations. The importance of methyl radicals in the reaction is firmly established,[4] but it was only recently shown[5] that methane is strongly adsorbed on a working Sm_2O_3 catalyst. Using isotope switching techniques and apparatus identical with that described previously,[5] we now report that gas-phase oxygen exchanges rapidly with the Sm_2O_3 lattice oxygen and, in the presence of methane under synthesis conditions, is transferred to the oxygenated reaction products. In this work, pure Sm_2O_3 was used as catalyst, all experiments being carried out after it had been on-stream for 30 min.

Examination of the results obtained for the oxygen isotope transients when $^{18}O_2$ replaced $^{16}O_2$ in helium or methane (10% O_2 in He or CH_4) reveals the following.

(1) For the O_2/He case a slow loss of $^{16}O_2$ and a slow rise of the $^{18}O_2$ were observed. Together with the long time required to return the $^{18}O_2$ and $^{18}O^{16}O$ signals to their background values after the end of the $^{18}O_2$ pulse (Figure 1 (parts a and b)), these results clearly indicate the uptake of large amounts of $^{18}O_2$ by an oxygen pool present in the catalyst. A lower limit estimate of 1×10^{21} atoms/g is made for the pool at this temperature from the integration of the area under the trailing parts of these curves, and its comparison with the area under the pulse whose duration and flow rate was accurately known. This value is nearly equal to the total number of oxygen atoms (5×10^{21} atoms/g) present in Sm_2O_3 and is consistent with data by Winter[6] who found that up to 1×10^{20} oxygen atoms/g are available for exchange in Sm_2O_3 at 400 °C. It is also noticeable that as the $^{16}O_2$ is replaced, the $^{16}O^{18}O$ formation slows as expected. Immediately after the return to $^{16}O_2$, a sharp spike in the $^{16}O^{18}O$ formation rate occurs, reflecting the exchange which has taken place in the mixed boundary between the two isotopic forms. Similar effects were observed previously.[5] As decay of the $^{18}O^{16}O$ formation rate continues long after $^{18}O_2$ has been replaced, the exchange must occur, at least partially, on the catalyst surface. The obvious differences in the decay rates of $^{18}O_2$ and $^{18}O^{16}O$ following the end of the $^{18}O_2$ pulse reflect the relative abundances of ^{18}O and ^{16}O on the catalyst surface.

(2) When the above experiments were carried out under synthesis conditions, i.e., with methane replacing helium, only small amounts of labeled oxygen appeared in the gas phase, because

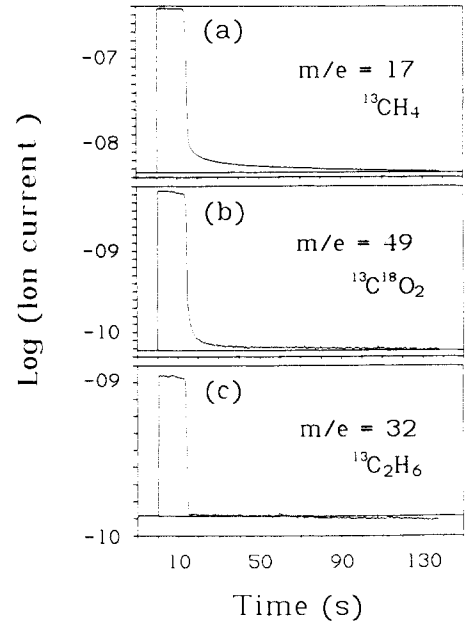

Figure 2. Trasients observed for $^{13}CH_4$, $^{13}C^{18}O_2$, and $^{13}C_2H_6$ when $^{13}CH_4$ replaced CH_4. $^{18}O_2$ was used to move the molecular weight of CO_2 to 48. Sm_2O_3 catalyst, 700 °C, 10% $^{18}O_2$ in CH_4, space velocity 4.7 l/min/g.

under these conditions almost complete oxygen consumption occurred. However, examination of the labeled carbon dioxide species (Figure 1 (parts c and d)) showed that their rates of decay after the end of the $^{18}O_2$ pulse approximately matched the desorption curves of the corresponding oxygen species. As the catalyst surface under synthesis conditions is expected to contain additional oxygen forms (e.g., OH^-, CO_3^{2-}, H_2O) such a result is not unreasonable.

(3) The CO_2 and C_2H_6 formation under synthesis conditions was also studied with $^{13}CH_4$. In this experiment, a $CH_4/^{18}O_2$ reactant mix was used to shift the CO_2 molecular weight to 48, away from any interference from propane which has a major fragmentation peak at the molecular weight of CO_2. A $^{13}CH_4$ pulse of the normal 14-s duration was then applied. As shown in Figure 2, the $^{13}C^{18}O_2$ pulse had the same shape as the labeled methane pulse. The incorporation of $^{13}CH_4$ into carbon dioxide is obviously very fast, and an identical result was obtained for the formation and decay of $^{13}C_2H_6$ in this experiment. This observation requires that the $^{13}CH_4$ converted to $^{13}CO_2$ did not first enter the large pool of CH_4 known to be present on the catalyst surface[5] and is in striking contrast to the tracing of $^{18}O_2$ to CO_2.

The preceding results are consistent with the following reaction scheme

Scheme I

$$O_2 + S \underset{\text{slow}}{\overset{\text{fast}}{\rightleftharpoons}} S^*O_2 \quad (1)$$

$$[P] + O_2 \xrightarrow{\text{fast}} CO \rightarrow CO_2 \quad (2)$$

$$^{\bullet}CH_3 + {}^{\bullet}CH_3 \xrightarrow{\text{fast}} C_2H_6 \quad (3)$$

in which oxygen atoms rapidly enter the lattice of the catalyst [S], the rate-determining step of the exchange being the desorption of molecular oxygen as was convincingly demonstrated for samarium and other catalysts by Winter.[6] Oxygen molecules also react with the precursors [P] of CO_2, perhaps to form initially CO, which is rapidly further oxidized. In view of the important role which methyl radicals are believed to play in the reaction,[4] this species may well be the CO_2 precursor. The scheme readily accounts for the striking difference observed for the $^{18}O_2$ and ^{13}C

(4) (a) Campbell, K. D.; Morales, E.; Lunsford, J. H. *J. Am. Chem. Soc.* **1987**, *109*, 7900. (b) Campbell, K. D.; Zhang, H.; Lunsford, J. H. *J. Phys. Chem.* **1988**, *92*, 750. (c) Labinger, L. A.; Ott, K. *J. Phys. Chem.* **1987**, *91*, 2682.

(5) Ekstrom, A.; Lapszewicz, J. A. *J. Chem. Soc., Chem. Commun.*, in press.

(6) (a) Winter, E. R. S. *J. Chem. Soc. A* **1969**, 1832. (b) Winter, E. R. S. *Ibid.* **1968**, 288.

transients but requires that the catalyst acts only as an oxygen sink as far as the CO_2 formation is concerned. The only other possibility appears to be that CO_2 formation occurs on catalyst sites to which oxygen is transferred slowly but CH_4 rapidly.

The role of the oxygen in the formation of the methyl radicals is more difficult to interpret at this time. It is a striking feature of the reaction that all product formation, both oxygenates and higher hydrocarbons, ceases instantly when helium replaces oxygen in the feed.[7] Furthermore, it appears from recent work[7] that the rate of lattice oxygen exchange determines the catalyst activity. These results seem to suggest that the lattice oxygen atoms themselves cannot be a significant source of reactant oxygen and that molecular, gas-phase oxygen is somehow involved. This aspect is currently under study in our laboratory. A similar and related aspect of this reaction is that the formation of all the reaction products is very fast compared to the time scale of the transients, while there is now convincing evidence that large amounts of methane are present on the catalyst which desorb much more slowly and which at present seem to have no obvious role in the reaction mechanism.[5] It is tempting to speculate that most of the chemistry involved occurs at the gas/solid interface, the only function of the catalyst being the production of reaction intermediates.

(7) Ekstrom, A.; Lapszewicz, J. A., unpublished observation.

Carbon Monoxide and Carbon Dioxide Carbon–Metal Bond Insertion Chemistry of Alkyliron(III) Porphyrin Complexes

Isam M. Arafa, Koo Shin, and Harold M. Goff*

Department of Chemistry, University of Iowa
Iowa City, Iowa 52242

Received January 4, 1988

Migratory insertion reactions represent one of the major classes of reactivity exhibited by organometallic species. In general, for metal–alkyl complexes, the process involves transfer of a cis ligand (such as CO) into a metal–carbon bond. Insertion reactions are also known for which prior coordination of the inserting group is not feasible. Among the reactions for which this "direct insertion" process is likely are the CO, isonitrile, aldehyde,[1] and alkene[2] insertions into hydridorhodium(III) porphyrins, and the light-driven CO_2 insertion into the methylindium(III) porphyrin complex.[3] Indirect evidence also exists for SO_2 insertion[4] and for dioxygen insertion[5] into an alkyliron(III) porphyrin bond. Metalloporphyrin derivatives are poor candidates for *migratory* insertion by virtue of the fact that cis ligation of two axial ligands is highly unfavorable. Accordingly, Halpern and co-workers have recently proposed a novel free radical mechanism for alkene insertion into Rh–Rh and Rh–H bonds of rhodium octaethylporphyrin.[2]

The first evidence is presented here for CO and CO_2 insertion reactions of alkyliron(III) porphyrin complexes. Spectroscopic results are consistent with generation of the respective acyl and carboxylatoiron(III) porphyrin complexes. An additional feature that renders this chemistry distinctly different than that of classical organometallic compounds is the paramagnetism of the iron(III) center in both the parent alkyl complex and in the insertion products.

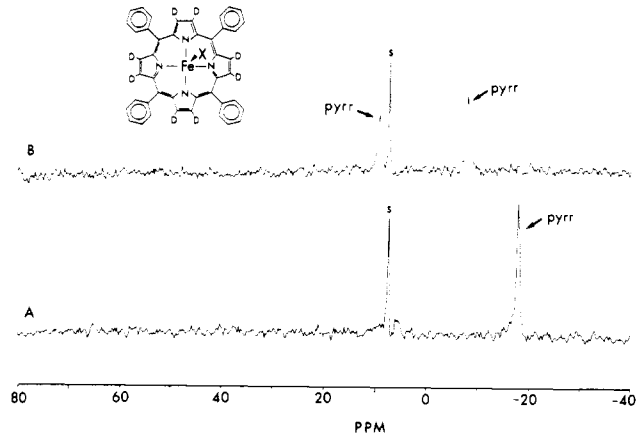

Figure 1. Deuterium NMR spectra of (TPP-d_8)Fe(III) species, 55 MHz, 25 °C, benzene solution, $(CD_3)_4Si$ reference. The deuterium pyrrole signals are denoted "pyrr", and the natural abundance solvent signal is labeled "s": (A) (TPP-d_8)FeBu and (B) product of (TPP-d_8)FeBu with CO.

Lithium alkyls were generated in hexane solution from the corresponding chlorinated hydrocarbon and lithium metal or, in the case of the *n*-butyl derivative, purchased (Aldrich) as a hexane solution. All reactions were performed in an inert atmosphere chamber filled with argon. Alkyliron(III) tetraphenylporphyrin complexes were prepared by combination of stoichiometric amounts of the lithium alkyl derivatives in hexane with a benzene or toluene solution of chloroiron(III) tetraphenylporphyrin ((TPP)FeCl) at a concentration of 2.0–5.0 mM.[6,7] In order to readily distinguish the pyrrole proton (deuterium) signal, it was most convenient to utilize (TPP-d_8)FeCl (deuteriated at the pyrrole positions). Formation of the alkyl complex was monitored by deuterium NMR spectroscopy, in which case the pyrrole deuteron signal at 79 ppm for the high-spin chloroiron(III) porphyrin was replaced by one in the −16 to −19 ppm region characteristic of the low-spin alkyliron(III) complex[6] as shown in Figure 1.

Insertion reactions were carried out under anaerobic conditions in NMR tubes. Carbon monoxide was gently bubbled through the benzene solution of the alkyliron porphyrin for 3–5 min, and an atmosphere of CO at ambient pressure was maintained in the septum-sealed tube. Optical spectra were recorded before and after the NMR measurements by removal of a small portion of the NMR sample inside the inert atmosphere chamber. Light was not required to effect the reactions.

Evidence for reaction between (TPP)Fe–alkyl and CO is found in changes for both optical and NMR spectra. Bands at 392, 412 (Soret), 518, and 552 nm for the red (TPP)FeBu complex[8] were replaced by bands at 406 (Soret), 513, 560, 603, and 637 nm upon equilibration with CO. The solution remained red in color. With CO addition the deuterium NMR spectrum for (TPP-d_8)FeBu with a pyrrole deuteron signal at −17.2 ppm was converted to one with a new pyrrole deuteron signal at −8.2 ppm (Figure 1). A second pyrrole signal at 8.7 ppm was attributable to the iron(II) porphyrin–carbon monoxide byproduct.[9] For solutions in which partial conversion had taken place, both −17.2 and −8.2 ppm

(1) (a) Wayland, B. B.; Woods, B. A. *J. Chem. Soc., Chem. Commun.* **1981**, 700. (b) Wayland, B. B.; Woods, B. A.; Pierce, R. *J. Am. Chem. Soc.* **1982**, *104*, 302. (c) Wayland, B. B.; Woods, B. A.; Minda, V. M. *J. Chem. Soc., Chem. Commun.* **1982**, 634.

(2) Paonessa, R. S.; Thomas, N. C.; Halpern, J. *J. Am. Chem. Soc.* **1985**, *107*, 4333.

(3) Cocolios, P.; Guilard, R.; Bayeul, D.; Lecomte, C. *Inorg. Chem.* **1985**, *24*, 2058.

(4) Cocolios, P.; Laviron, E.; Guilard, R. *J. Organomet. Chem.* **1982**, *228*, C39.

(5) Arasasingham, R. D.; Balch, A. L.; Latos-Grazynski, L. *J. Am. Chem. Soc.* **1987**, *109*, 5846.

(6) Cocolios, P.; Lagrange, G.; Guilard, R. *J. Organomet. Chem.* **1983**, *253*, 65.

(7) Insertion results were identical for in situ generated or recrystallized alkyliron(III) porphyrins.

(8) (a) Lexa, D.; Mispelter, J.; Saveant, J.-M. *J. Am. Chem. Soc.* **1981**, *103*, 6806. (b) Guilard, R.; Lagrange, G.; Tabard, A.; Lancon, D.; Kadish, K. M. *Inorg. Chem.* **1985**, *24*, 3649.

(9) The iron(II) product, (TPP)Fe(CO), presumably results from homolytic rupture of the iron(III)–alkyl bond with loss of the alkyl radical from the solvent cage and subsequent coordination of CO by the iron(II) product. Addition of α-(4-pyridyl 1-oxide)-*N*-*tert*-butylnitrone to the reaction mixture yielded a "trapped" alkyl radical species detectable by ESR spectroscopy. In benzene solution the insertion product predominates, whereas in the highly solvating THF solvent the iron(II) carbonyl species is the major product.

0002-7863/88/1510-5228$01.50/0